

Patterned Supported Lipid Bilayers and Monolayers on Poly(dimethylsiloxane)

Peter Lenz,^{*,†,‡} Caroline M. Ajo-Franklin,[‡] and Steven G. Boxer[‡]

Lyman Laboratory of Physics, Harvard University, Cambridge, Massachusetts 02138, and
Department of Chemistry, Stanford University, Stanford, California 94305-5080

Received June 23, 2004. In Final Form: September 6, 2004

A simple and practical method for patterning supported lipid bilayers on poly(dimethylsiloxane) is presented. By using electron microscopy grids to laterally control the extent of plasma oxidation, the substrate is partitioned into regions of different hydrophilicities. Addition of vesicles then results in the spontaneous formation of lipid bilayers and monolayers side-by-side on the surface, separated by regions that contain no lipid and/or a region with adhering vesicles. By using millimeter-sized plastic masks we are able to control the formation of these lipid structures on macroscopic patches by simply varying the plasma-cleaning time. For the first time, we are able to influence, in a controlled fashion, the chemical composition of a substrate in such a way that it supports fluid lipid monolayers, rejects lipid adhesion, adsorbs intact lipid vesicles, or supports fluid bilayers.

1. Introduction

Supported membranes on solids are an excellent model system for biomembranes with potential for both scientific and technological applications.^{1,2} They provide a self-assembled system to incorporate and localize biological components and can serve as an interface between inorganic materials and biological systems. Lipids in supported membranes exhibit the lateral fluidity of free lipid membranes and show similar thermodynamic and structural properties. As a result of the close proximity of the supported membrane to a solid surface, a variety of sophisticated surface-sensitive techniques can be used which are not applicable to free membranes. Furthermore, cells recognize components incorporated into the supported membrane.^{3–6} Thus, supported bilayers provide a well-defined environment in which interactions between cells, vesicles, and proteins can be investigated systematically.

For many purposes it is essential to control the formation and composition of the supported membrane. This can be achieved by laterally structuring the lipid bilayers.⁷ A variety of techniques have been developed for patterning supported bilayers ranging from lithographic methods^{7–9} and microcontact printing,^{10–12} where the substrate is appropriately modified, to blotting¹³ and polymer lift-off

procedures,¹⁴ where the bilayer itself is modified. In all cases a fluid membrane is partitioned into compartments, which are separated by barriers restricting the lateral diffusion of the lipids. These structures can be used to modify the local chemical composition of the membrane, to parallelize measurements on the membrane, and even to control cell–cell and cell–surface interactions.¹⁵ These techniques could also find important practical applications.

Despite the widespread use of supported bilayers and patterned supported bilayers, there is a poor understanding of what surface properties are responsible for the self-assembly of fluid bilayers and what surface properties are responsible for barrier regions. Fully fluid supported bilayers are known to form by vesicle fusion only on highly hydrophilic mica,¹⁶ silica solid surfaces (i.e., glass, quartz, thermally grown silicon dioxide, and sputtered silicon dioxide),^{3,17} and oxidized poly(dimethylsiloxane) (PDMS),¹⁸ which displays a SiO_x surface.¹⁹ In contrast, exposure of lipid vesicles to many other hydrophilic solid surfaces results in lipid structures other than a fully fluid bilayer.^{17,20–22} Recent approaches to elucidate the relevant parameters include systematic tuning of surface free energy using homogeneous binary mixtures of self-assembled monolayers (SAMs),²³ tuning of surface charge and polarity using pH, monovalent, and divalent ions,^{24,25} and tuning of hydrophilic–hydrophobic edge affects by varying patterned SAM geometries.²⁶ In an orthogonal approach, Richter et al.²⁷ have varied vesicle composition

* To whom correspondence should be addressed. E-mail: peter.lenz@physik.uni-marburg.de.

† Harvard University.

‡ Stanford University.

(1) Sackmann, E. *Science* **1996**, *271*, 43.

(2) Boxer, S. G. *Curr. Opin. Chem. Biol.* **2001**, *4*, 704.

(3) Brian, A. A.; McConnell, H. M. *Proc. Natl. Acad. Sci. U.S.A.* **1984**, *81*, 6159.

(4) Tamm, L. K.; McConnell, H. M. *Biophys. J.* **1985**, *47*, 105.

(5) Graukoui, A.; Bromley, S. K.; Sumen, C.; Davis, M. M.; Shaw, A. S.; Allen, P. M.; Dustin, M. L. *Science* **1999**, *285*, 221.

(6) Groves, J. T.; Dustin, M. L. *J. Immunol. Methods* **2003**, *278*, 19.

(7) Groves, J. T.; Ulman, N.; Boxer, S. G. *Science* **1997**, *275*, 651.

(8) van Oudenaarden, A.; Boxer, S. G. *Science* **1999**, *285*, 1046.

(9) Morigaki, K.; Baumgart, T.; Offenhäusser, A.; Knoll, W. *Angew. Chem., Int. Ed.* **2001**, *40*, 172.

(10) Jenkins, A. T. A.; Bushby, R. J.; Boden, N.; Evans, S. D.; Knowles, P. F.; Liu, Q. Y.; Miles, R. E.; Ogier, S. D. *Langmuir* **1998**, *14*, 4675.

(11) Kung, L. A.; Kam, L.; Hovis, J. S.; Boxer, S. G. *Langmuir* **2000**, *16*, 6773.

(12) Srinivasan, M. P.; Ratto, T. V.; Stroev, P.; Longo, M. L. *Langmuir* **2001**, *17*, 7951.

(13) Hovis, J. S.; Boxer, S. G. *Langmuir* **2000**, *16*, 894.

(14) Orth, R. N.; Kameoka, J.; Zipfel, W. R.; Ilic, B.; Webb, W. W.; Clark, T. G.; Craighead, H. G. *Biophys. J.* **2003**, *85*, 3066.

(15) Kam, L.; Boxer, S. G. *J. Biomed. Mater. Res.* **2001**, *55*, 487.

(16) Mou, J. X.; Yang, J.; Shao, Z. F. *J. Mol. Biol.* **1995**, *248*, 507.

(17) Keller, C. A.; Kasemo, B. *Biophys. J.* **1998**, *75*, 1397.

(18) Hovis, J. S.; Boxer, S. G. *Langmuir* **2001**, *17*, 3400.

(19) Hillborg, H.; Gedde, U. W. *IEEE Trans. Dielectr. Electr. Insul.* **1999**, *6*, 703.

(20) Rädler, J.; Strey, H.; Sackmann, E. *Langmuir* **1995**, *11*, 4539.

(21) Groves, J. T.; Ulman, N.; Cremer, P. S.; Boxer, S. G. *Langmuir* **1998**, *14*, 3347.

(22) Reimhult, E.; Höök, F.; Kasemo, B. *Langmuir* **2003**, *19*, 1681.

(23) Silin, V. I.; Wieder, H.; Woodward, J. T.; Valincius, G.; Offenhäusser, A.; Plant, A. L. *J. Am. Chem. Soc.* **2002**, *124*, 14676.

(24) Cremer, P. S.; Boxer, S. G. *J. Phys. Chem. B* **1999**, *103*, 2554.

(25) Ekeröth, J.; Konradsson, P.; Höök, F. *Langmuir* **2002**, *18*, 7923.

(26) Jenkins, A. T. A.; Bushby, R. J.; Evans, S. D.; Knoll, W.; Offenhäusser, A.; Ogier, S. D. *Langmuir* **2002**, *15*, 3176.

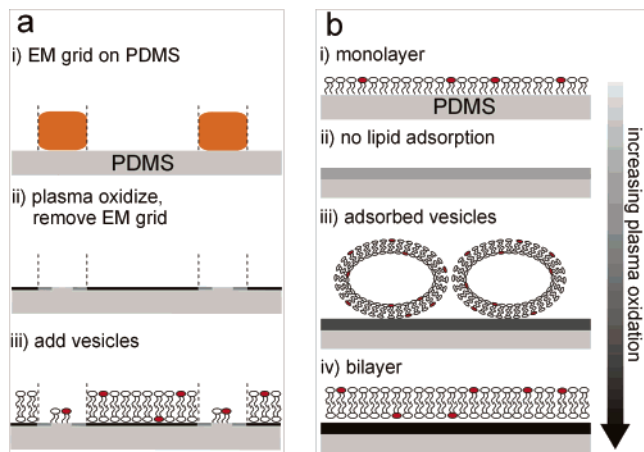


Figure 1. (a) Schematic illustration of the supported bilayer patterning method. (i) An EM-grid is placed on the PDMS substrate and (ii) exposed to air plasma creating hydrophilic (shown as a black line) and hydrophobic (light gray) regions. The hydrophilic parts of the substrate are below the holes of the mask. During plasma oxidation not only a chemical modification but also a topographical change takes place; this is schematically shown in Figure 4e. The hydrophobic and hydrophilic regions are separated by a gap region (medium gray) of mixed surface chemistry. (iii) Upon addition of vesicles, bilayers are formed on the unmasked parts whereas monolayers are formed on the masked parts of the substrate. Both regions are separated by the gap region in which no lipids adhere. (b) Schematic illustration of the dependence of the supported lipid phase on the plasma oxidation time. (i) Fluid supported monolayers form on unmodified PDMS, while (ii) a small degree of plasma modification results in a surface that rejects lipid assembly (gap region). (iii) Further plasma oxidation of the surface causes vesicles to adsorb, ultimately leading to (iv) formation of a fluid supported bilayer.

to show that, for silica surfaces, the net charge of the vesicle determines the resulting lipid structure. Nonetheless, a complete picture of the facets governing supported bilayer formation has not emerged.

In the following we describe a simple technique for creating patterned bilayers on PDMS surfaces. In earlier work it was found that supported bilayers can be formed on plasma-oxidized PDMS (SiO_x) surfaces, whereas monolayers appear to form on unprocessed, hydrophobic PDMS ($-\text{SiCH}_3$ terminated) surfaces.¹⁸ In the new method, we laterally control the surface chemistry of PDMS by partially covering a hydrophobic PDMS substrate with suitable masks; see Figure 1a for a schematic illustration. Under appropriate plasma oxidation conditions, large areas of the PDMS substrate are partitioned into hydrophilic SiO_x and hydrophobic $-\text{SiCH}_3$ terminated surface regions. The hydrophobic regions are those parts of the substrate that were covered by the mask during plasma oxidation, while the hydrophilic regions correspond to the location of the holes of the mask. Self-assembly of supported bilayers by fusion of unilamellar vesicles yields a patterned bilayer on the hydrophilic regions that have the geometry of the inverse grid. The size and geometry of the corresponding lipid domains can be easily varied, with sizes ranging from a few micrometers up to several millimeters by using commercially available electron microscopy grids (EM-grids) as masks. Thus, this method involves no investment in lithographic equipment and can be rapidly applied to pattern surfaces. As described below, the intermediate degree of surface oxidation at the edge of the mask pattern rejects lipid self-assembly, the

region that is fully shadowed by the mask allows self-assembly of a lipid monolayer, and the region that is fully oxidized allows the formation of fluid lipid bilayers (see Figure 1b for a schematic illustration). Contact angle measurements provide a direct correlation between the PDMS surface chemistry and formation of these different lipid phases. These observations suggest that the proportion of silanol to silane groups is a key parameter in the formation of various supported lipid phases.

2. Experimental Section

Small unilamellar vesicles (SUVs) were prepared from egg phosphatidylcholine (eggPC, Avanti Polar Lipids) with varying mol % Texas Red 1,2-dihexadecanoyl-*sn*-glycero-3-phosphoethanolamine, triethylammonium salt (Texas Red DHPE, Molecular Probes), and varying mol % NBD 1-palmitoyl-2-[12-[(7-nitro-2-1,3-benzoxadiazol-4-yl)amino]dodecanoyl]-*sn*-glycero-3-phosphocholine (NBD PC, Avanti Polar Lipids). The hydrophobic tails of lipids in an eggPC mixture are mainly palmitoyl (16:0) and oleyl (18:1) groups. The lipids were mixed together in chloroform, dried under N_2 , put under a vacuum for at least 2 h, resuspended with Millipore (18 M Ω) water, and extruded 19 times through polycarbonate membranes of 50-nm pore diameter (Avanti Extruder). To make carboxyfluorescein (CF) content-labeled vesicles, the lipids were resuspended in 20 mM CF (Molecular Probes) buffered in 50 mM phosphate at pH 7.3, extruded through polycarbonate membranes as described above, and then isolated using a Sepharose CL-4B size-exclusion column. The resulting lipid vesicles were diluted with buffer (10 mM phosphate, 100 mM NaCl at pH 7.3) to ~ 1 mg/mL immediately before use. The results described below were independent of the vesicle composition used.

Flat PDMS substrates were formed by curing Sylgard 182 or 184 (Dow Corning) on planar silicon wafers for 80 min at 70 °C. To pattern the oxidation of PDMS surfaces with different pattern and mesh size EM-grids [Gilder Grids from Electron Microscopy Sciences and Ernest F. Fullam Lab, Athene Grids from Ted Pella, and VECO Grids from Electron Microscopy Sciences], the masks were pressed on the PDMS substrate by using tweezers (slight hand pressure). To pattern PDMS substrates with circular 5-mm-diameter polypropylene masks, the surface was simply covered with the mask without additional pressure. The masked PDMS surface was placed for 0–120 s into a plasma cleaner (model PDC-3xG, Harrick Scientific) under high power (30 W) with a small amount of air leaking into the chamber. To achieve consistent patterning, it was important to place the PDMS substrate in the same location with respect to the electrodes in the plasma cleaner. After plasma exposure, the polypropylene masks showed no tendency to adhere to the PDMS surface, while the EM-grids frequently stuck to the surface. In both cases, after removal of the mask the PDMS surface is not noticeably deformed. After removal of the mask, a small droplet containing vesicles was put onto the PDMS substrate for 30–60 s. The excess vesicles were washed away with large amounts of water or buffer, and the whole system was assembled under water into a thin sandwich covered by a glass coverslip separated by spacers.

The surfaces were imaged with a Nikon E800 epifluorescence microscope. Atomic force microscopy (AFM) was used to probe the patterned surface topography (Multimode AFM-2 by Digital Instruments). Images of the patterned PDMS in air (before addition of vesicles) were recorded in tapping mode using Nanoprobe SPM tips with nominal spring constants of 350 kHz at scanning rates of 1 Hz.

To correlate contact angle and supported lipid phase, an approximately 2 mm \times 2 mm area that had only the lipid phases was located using fluorescence microscopy. This area was exposed to air and rinsed in absolute methanol for 5 s to remove the lipids, and then the contact angle was determined with a goniometer (First Ten Angstroms FTA 200) at room temperature and ambient humidity using Millipore water. Sessile drop measurements were made by lowering an ~ 0.25 – 0.5 μL drop of water onto the surface using 2 \times magnification. The contact angle was measured within 2 min of lowering the drop onto the surface. Because the measured contact angle did not change over 4 min, no correction for evaporation was made. The data represent a

(27) Richter, R.; Mukhopadhyay, A.; Brisson, A. *Biophys. J.* **2003**, *85*, 3035.

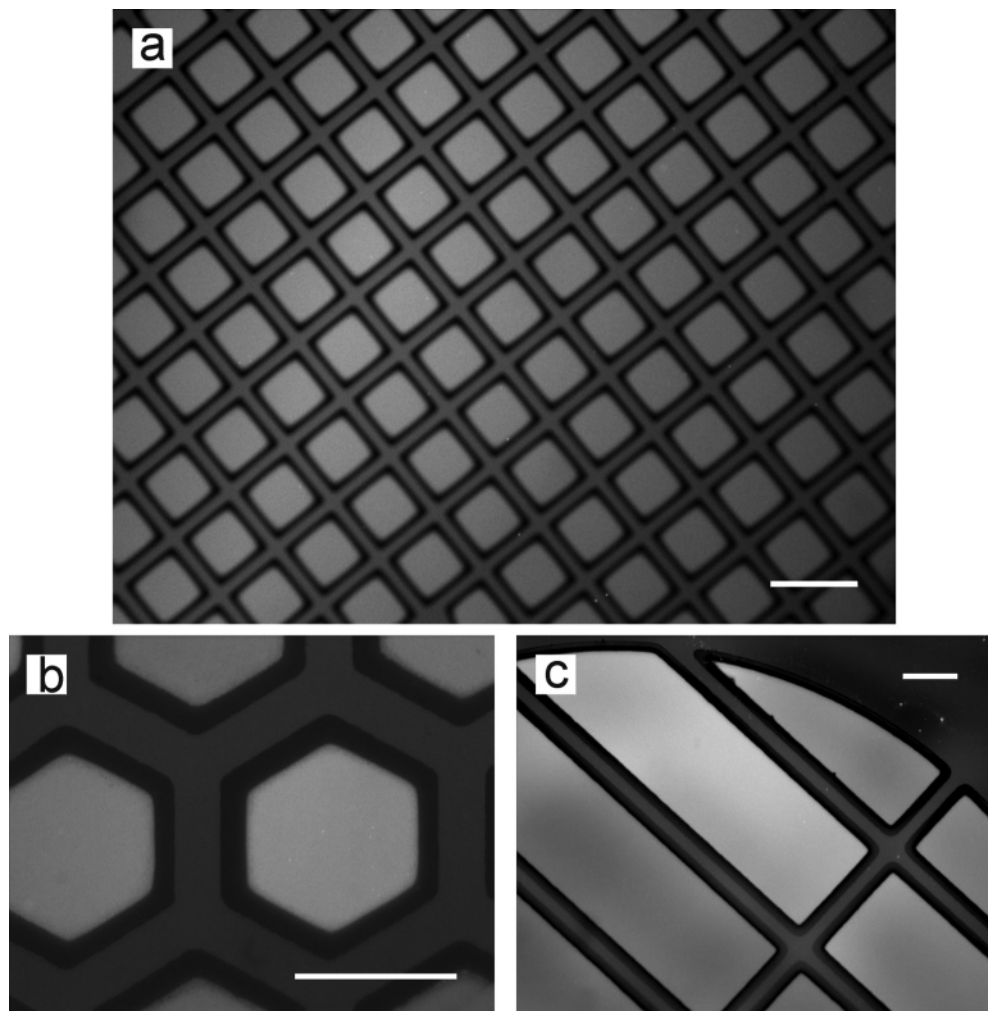


Figure 2. (a) Epifluorescence image of a patterned bilayer (eggPC with 1 mol % Texas Red DHPE) on 184-PDMS. The bilayer has the inverse geometry of the EM-grid (300 mesh Standard Square Gilder Grid, Ernest F. Fullam Lab). The regions which were covered by the EM-grid appear as somewhat darker lines in the image, whereas the brighter squares correspond to the location of the holes. Both regions are fluorescent from the Texas Red labeled lipids, and they are separated by a gap region showing no fluorescence. The dimensions of the image are $894\ \mu\text{m} \times 703\ \mu\text{m}$; the scale bar is $100\ \mu\text{m}$. The width of the darker lines is $14\ \mu\text{m}$, the squares have a size of $56\ \mu\text{m}$, and the periodicity of the grid is $83\ \mu\text{m}$. To illustrate the generality of our technique, we have produced domains shaped as hexagons (b) and as millimeter channels (c). The dimensions of image b are $150\ \mu\text{m} \times 118\ \mu\text{m}$; the scale bar is $50\ \mu\text{m}$. The dimensions of image c are $894\ \mu\text{m} \times 703\ \mu\text{m}$; the scale bar is $100\ \mu\text{m}$. In the last two cases, we have used 184-PDMS and grids from Electron Microscopy Sciences.

range of at least three measurements for each surface. Fluorescence microscopy indicated that this washing procedure removes more than 99% of the fluorescent lipids. A comparison of the contact angles of untreated PDMS and oxidized PDMS in the absence and presence of a 5 s methanol rinse indicates that the contact angle of either surface is not affected by the methanol rinse.

3. Results and Discussion

Figure 2 shows epifluorescence images of a patterned bilayer (eggPC with 1 mol % Texas Red DHPE) created as described above with 15 s of plasma exposure. These patterns covered wide regions of the PDMS substrate and were stable for hours. In Figure 2a a square grid has been used to structure the oxidation of the PDMS surface; for this mask the masked regions all are connected while the unmasked regions are spatially separated. As can be seen directly from the image, both the masked and unmasked regions have lipids adsorbed; however, the unmasked regions appear brighter than the masked regions. The unmasked and masked regions are separated by dark regions, which we call gap regions. As illustrated in Figure 2b,c, many other shapes on various length scales can be

readily fabricated on the PDMS surface, all leading to the assembly of a bright region where the surface was accessible to plasma, a less bright region where the surface oxidation was mitigated by the mask, and a dark intervening gap region.

In earlier work, it was shown that a fluid bilayer assembles on PDMS oxidized for 1–2 min under similar conditions.¹⁸ The bilayer composition was demonstrated by extracting the lipids from a defined area on the surface and performing quantitative fluorescence analysis, and the fluidity was demonstrated by performing fluorescence recovery after photobleaching measurements.¹⁸ The unmasked bright regions are uniformly fluorescent under $60\times$ magnification and recover fully after spot photobleaching. Fluorescence quenching experiments provide an additional indication that a bilayer is present on the surface; half the fluorescence intensity, corresponding to the fluorophores in the top leaflet, is quenched upon addition of a quencher into bulk solution. Therefore, we conclude that these regions are covered by fluid supported bilayers. Taking the intensity in the bright region as representative of a bilayer, the intensity ratio between

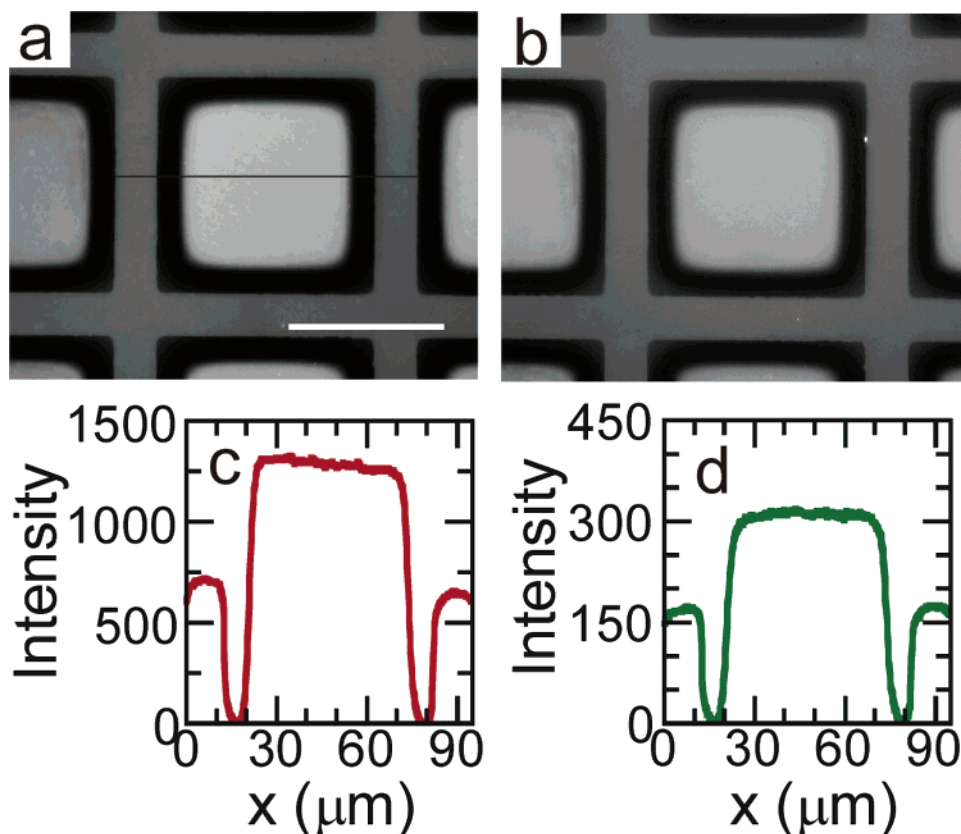


Figure 3. Magnified view of a patterned bilayer (eggPC with 0.5 mol % Texas Red and 1 mol % NBD) on 184-PDMS created with the same EM-grid as the substrate in Figure 2a. Images a and b show the fluorescence from the Texas Red labeled lipids and from the NBD-labeled lipids, respectively. The intensity profiles of the Texas Red signal (c) and of the NBD signal (d) are both measured along the line drawn in part a. The dimensions of images a and b are $150 \mu\text{m} \times 118 \mu\text{m}$; the scale bar is $65 \mu\text{m}$.

the unmasked and masked regions (cf., e.g., Figures 2 and 3) is consistent with a monolayer of lipids in the masked region. Figure 3c,d shows intensity profiles of the masked and unmasked patches for the 0.5% Texas Red DHPE and 1% NBD PC composition measured along the line drawn in Figure 3a. After subtraction of the background level, we find a ratio r of hydrophobic to hydrophilic intensities $r \approx 0.54$ for the Texas Red signal and $r \approx 0.57$ for the NBD signal.²⁸ Because the unmasked regions are uniformly fluorescent under $60\times$ magnification and recover fully after spot photobleaching and, upon addition of a fluorescence quencher, their fluorescence intensity drops to the background level, we conclude a fluid monolayer is formed over these regions. This observation, together with the observation that a fluid monolayer assembles on unmodified PDMS,¹⁸ suggests that the mask restricts plasma oxidation over covered regions.

The gap separating the bilayer and monolayer regions of the substrate is a novel feature of this patterning method. As seen in Figures 2 and 3, a nonfluorescent gap occurs for all the investigated patterning geometries, even

for systems with extended border regions. Photobleached patterns remained confined in the monolayer or bilayer regions, so no material exchange occurs across the gap region. In the gap region, the fluorescence intensity drops to the background level (Figure 3), so we conclude that no lipids are present in this region.

Because lipid adhesion and spreading can be prevented by large surface roughness,^{24,30} one possible explanation of the existence of gap regions on the patterned PDMS substrate is that these regions have rough topography. To determine if this was the case, we performed AFM studies of patterned PDMS substrates in the absence of any lipids (with the same EM-grids as in Figure 3); see Figure 4. As can be seen from these images the PDMS substrate is perfectly flat almost everywhere, except for a few localized defects and a narrow region around the boundary of the unmasked and masked regions. There, the substrate exhibits large peaks (with a height up to 100 nm). Although plasma oxidation does not affect the surface roughness of nonmasked PDMS,³¹ it appears that during the patterning process some mass transport takes place; see Figure 4b. A comparison of Figure 3 and Figure 4 shows that the shape and width of the monolayer is very similar to the shape and width of the region between the two peaks. Therefore, the border of the monolayer coincides with the peaks of the AFM image (see Figure 4e). The width of the EM-grid (i.e., the bar which corresponds to

(28) To check this interpretation, we have varied the composition of the bilayer in a series of experiments with mixtures containing n mol % head labeled lipids (Texas Red DHPE) and m mol % tail labeled lipids (NBD PC), with $(n, m) = (1, 0)$, $(n, m) = (2, 0)$, $(n, m) = (0.5, 1)$, $(n, m) = (1, 1)$, and $(n, m) = (0, 1)$. For all combinations, the unmasked regions were always brighter than the masked regions, and the regions were separated by dark gaps. For all vesicle compositions the measured intensity of the hydrophobic regions was, after subtraction of the background level, roughly half the intensity of the hydrophilic regions. Note that Texas Red headgroup labeled lipids are negatively charged and may tend to be mostly present in the upper leaflet of the bilayer.²⁹ If this is true, the intensity ratio between the monolayer and bilayer region is still expected to be about 1:2, so long as the Texas Red concentration is below a self-quenching concentration.

(29) Provencal, R. A.; Ruiz, J. D.; Parikh, A. N.; Shreve, A. P. *Biophys. J.* **2001**, *80*, 423A.

(30) Nissen, J.; Jacobs, K.; Rädler, J. O. *Phys. Rev. Lett.* **2001**, *86*, 1904.

(31) Hillborg, H.; Ankner, J. F.; Gedde, U. W.; Smith, G. D.; Yasuda, H. K.; Wikström, K. *Polymer* **2000**, *41*, 6851.

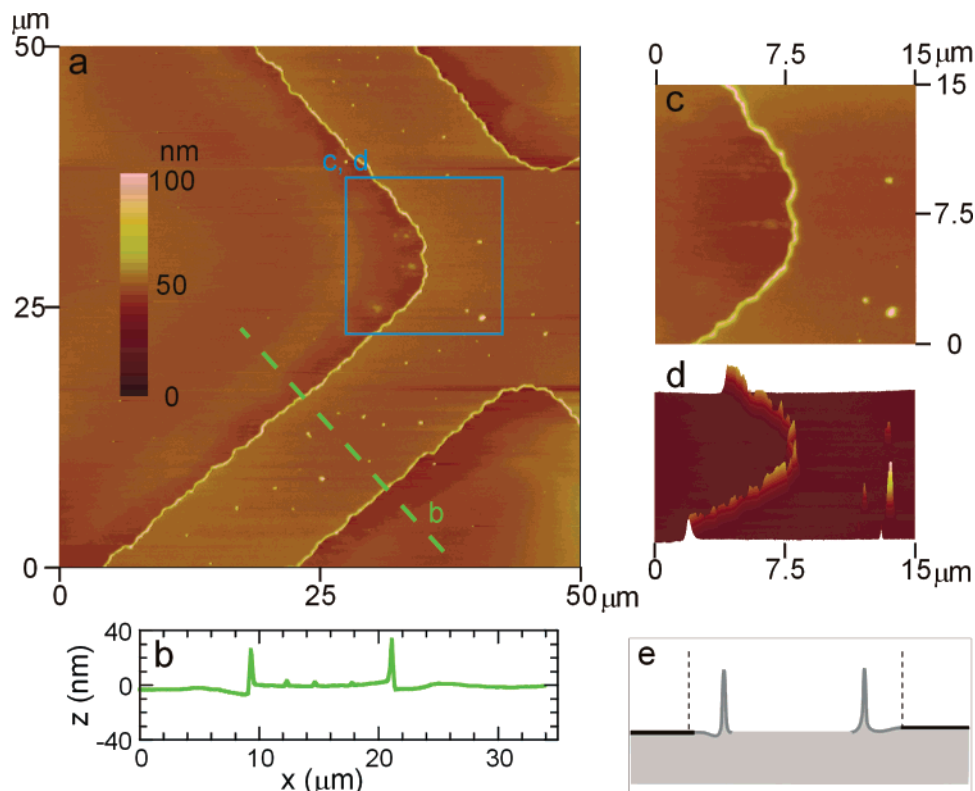


Figure 4. AFM image of a 184-PDMS substrate which has been patterned with the same EM-grid as the system presented in Figure 2a. The measurement has been performed on the plain substrate in air and in the absence of any lipids. (a) $50 \mu\text{m} \times 50 \mu\text{m}$ height image of the PDMS substrate. (b) Line profile over the region of induced roughness. (c) Zoom-in on the corner of a hydrophilic square corresponding to the gap region. (d) Three-dimensional view along the gap region. (e) Schematic diagram of the position of the topographical change in relation to the border of the EM-grid mask (the dashed lines), monolayer regions (light gray), gap regions (medium gray), and bilayer regions (black). This positioning is assigned by comparing the patterned topography of the PDMS surface, the pattern of the EM-grids, and the pattern of the monolayer, gap, and bilayer regions.

the mask part), $25 \mu\text{m}$, is larger than the width of the monolayer ($14 \mu\text{m}$), while it matches exactly the distance between the edges of adjacent bilayer patches ($25 \mu\text{m}$). Thus, the gap region is covered by the EM-grid during plasma oxidation, and it extends approximately $5.5 \mu\text{m}$ out from the peaks in each direction (Figure 4e). The peaks are approximately $0.5 \mu\text{m}$ wide and contain a relatively steep topography (slope > 0.10). This topography could be responsible for the absence of lipid adhesion,¹⁸ but the surrounding $5.0 \mu\text{m}$ region is smooth enough to allow lipid adhesion (slope ~ 0.02). Thus, the fact that no lipids adhere over the entirety of the gap region cannot be explained solely by roughness.

Alternatively, it has been shown that incompatible surface chemistry can block lipid adhesion to surfaces.^{11,21} Because it is well-known that exposure to air plasma alters the surface chemistry of PDMS,^{19,32–33} we hypothesized that the gap region could be caused by partial plasma oxidation leading to an intermediate surface chemistry.³⁴ We reasoned that if the mask would slow the rate of plasma oxidation and partial plasma oxidation was responsible for the formation of gap regions, then the presence of the gap region should be sensitive to the plasma oxidation time. Figure 5 shows the results after 0, 15, 30, and 60 s of plasma exposure to the EM-grid covered PDMS substrates followed by addition of eggPC with 1% Texas Red DHPE vesicles. Figure 5a shows that no plasma exposure of a masked PDMS surface results in a sample displaying uniform fluorescence corresponding to a ho-

mogeneous monolayer. After 60 s of plasma exposure, uniform fluorescence corresponding to that of a homogeneous bilayer was observed on the PDMS surface; see Figure 5d. This finding suggests that the mask only slows the rate of plasma oxidation by reducing the plasma exposure to covered regions. Figure 5b shows again that 15 s of plasma cleaning time leads to three levels of intensity corresponding to bilayer, monolayer, and gap regions. In contrast, after 30 s of plasma treatment the regions covered by the EM-grid are completely transformed into gap regions, while a supported bilayer extends across the unmasked regions. Therefore, when the plasma oxidation time is increased from 15 to 30 to 60 s, the regions that initially form supported monolayers become gap regions followed by supported bilayer regions. We observed this phenomenon with multiple grid shapes for various cleaning times. This sequence suggests time-dependent surface modification progressing from the edge of the mask to the interior.

(34) It is possible that the chemical residues could be deposited from the EM-grid and that this change in the surface chemistry of PDMS could be responsible for the formation of gap and adsorbed vesicle regions. To control the placement and removal of the mask, EM-grids were placed and removed on PDMS without plasma oxidation. Upon addition of vesicles only uniform fluorescence corresponding to a monolayer was observed. In an additional control experiment, a PDMS substrate was plasma cleaned without a mask for 60 s. Then the substrate was covered with a mask, plasma oxidized for an additional 15 s, and exposed to vesicles. If exposure of the mask to the plasma causes deposition of residue leading to the formation of gap regions, then this procedure should produce gap regions. Instead, no gap or adsorbed vesicle regions were observed to form on this doubly oxidized surface; only fluid supported bilayers formed. Taken together, these observations suggest that the chemical nature of the EM-grid is not responsible for the formation of gap regions.

(32) Hollahan, J. R.; Carlson, G. L. *J. Appl. Polym. Sci.* **1970**, *14*, 2499.

(33) Hillborg, H.; Sandelin, M.; Gedde, U. W. *Polymer* **2001**, *42*, 7349.

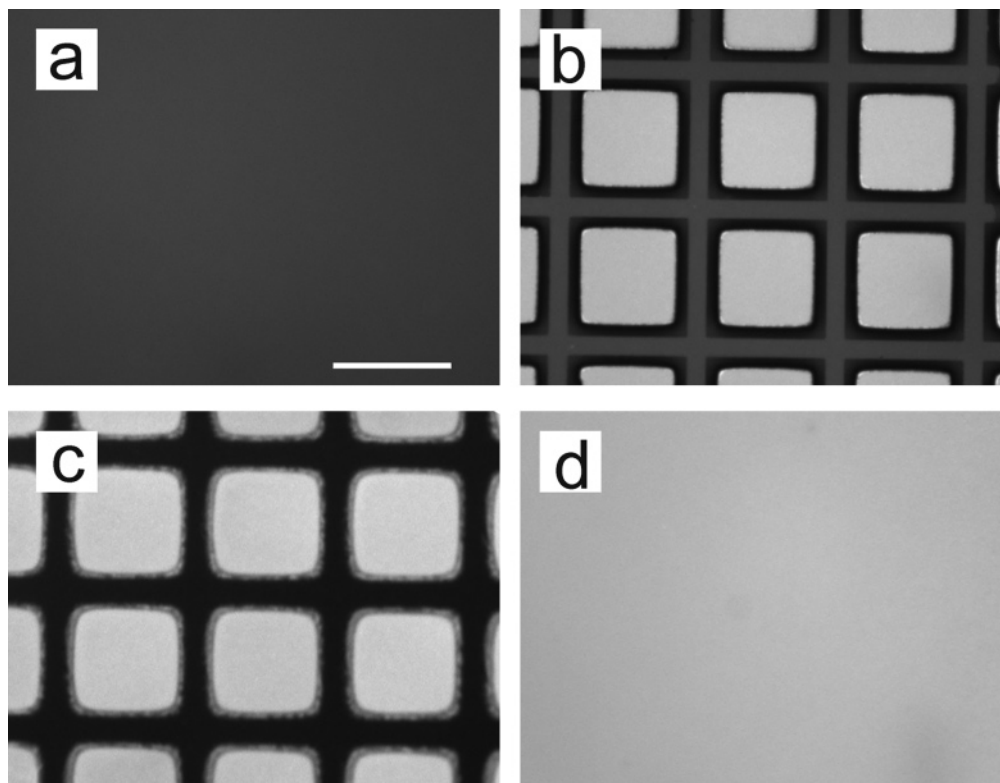


Figure 5. (a–d) Epifluorescence images of patterned supported lipid phases (eggPC with 1.0 mol % Texas Red DHPE) on variably oxidized 184-PDMS surfaces masked with 300 mesh EM-grids. (a) A fluid supported monolayer forms over the entire surface with 0 s of oxidation treatment. (b) After ~ 15 s of plasma oxidation, bilayer regions span the unmasked regions (bright squares), monolayers are present on the masked regions (gray grid lines), and gap regions (dark borders) form in between. (c) Upon ~ 30 s of plasma oxidation, gap regions cover the masked regions (dark grids), and again fluid supported bilayers (bright squares) are present over the unmasked regions. Additionally, adsorbed vesicles (bright punctate objects) are found between the bilayer and gap regions. (d) After ~ 60 s of exposure to air plasma, a supported bilayer is formed across the surface. The scale bar is $75 \mu\text{m}$.

A further indication that masking leads to gradual surface modification is the fact that we observed adhering, intact Texas Red-labeled vesicles with a content dye (CF) whose localization depended systematically on plasma oxidation time. Adsorbed intact SUVs were identified by their punctate appearance in both lipid-labeled (Texas Red DHPE) and content-labeled (CF) channels under high magnification and their extremely limited recovery after spot photobleaching ($<5\%$). For short plasma oxidation times (5 s), they appeared in the unmasked regions in the absence of a bilayer (data not shown). For intermediate times (20–30 s), vesicles frequently appeared as a ring between the gap region and the bilayer (see, e.g., Figure 5c). Spot photobleaching of the bilayer showed that the vesicles and bilayer were noncontiguous. Taken altogether, these observations suggest that increasing chemical modification of PDMS, dependent on the time exposed to plasma and accessibility to plasma (i.e., the distance from the EM-grid edge), results in a progression of supported lipid phases: supported monolayers, no lipid adhesion (gap), intact adsorbed vesicles, and supported bilayers.

Air plasma oxidation alters the wetting behavior of the PDMS surface from hydrophobic (contact angle $\sim 108^\circ$) to hydrophilic (contact angle $< 20^\circ$).^{32–33} To our knowledge, it has not been reported that restricted plasma exposure leads to surface chemistry of intermediate hydrophilicity. To test this hypothesis, we covered PDMS substrates with much larger nonmetal masks (5-mm-diameter polypropylene circles) and exposed them to plasma for varying amounts of time. When a masked PDMS and bare PDMS substrate are exposed to air plasma in parallel, a polypropylene-masked PDMS substrate has a larger contact angle (i.e., is more hydrophobic) than the nonmasked substrate.

Additionally, the contact angle at the center of the masked region is larger than the contact angle at the edge of the mask, and the contact angle of a given region decreases with increasing plasma exposure.³⁵ These observations confirm that masking of a PDMS substrate retards plasma oxidation in a spatially dependent way and indicates that surfaces of PDMS of intermediate hydrophilic/hydrophobic character can be formed in this manner.

As with the EM-grids, polypropylene masks can be used to pattern different supported lipid phases on PDMS by tuning the plasma cleaning time. However, with these masks it is possible to create lipid phases that extend over surface regions of many square millimeters. After masking a PDMS substrate with a polypropylene circle, exposing it to air plasma for 30 s, and adding eggPC with 1% Texas Red DHPE vesicles, the surface was patterned with gap regions and supported bilayer regions on the masked and unmasked regions, respectively (see Figure 6a). Typically, a supported bilayer was present on the unmasked regions, except for very short plasma treatment times in which adsorbed vesicles were present (data not shown). As shown in Figure 6, the supported lipid structure formed over the masked area was controlled by the time of plasma oxidation. Lipid monolayers (Figure 6b), gap regions (Figure 6c), adhering vesicles (Figure 6d), and lipid bilayers (Figure 6e) are respectively formed with increasing oxidation times (approximately 5, 30, 45, and 120 s) on the masked region on the PDMS substrate. Using the criteria discussed previously, these different supported lipid structures were identified by their recovery after

(35) With sufficiently long plasma oxidation times, on the order of tens of minutes, the center of a masked PDMS substrate can be rendered equally hydrophilic as nonmasked oxidized PDMS.

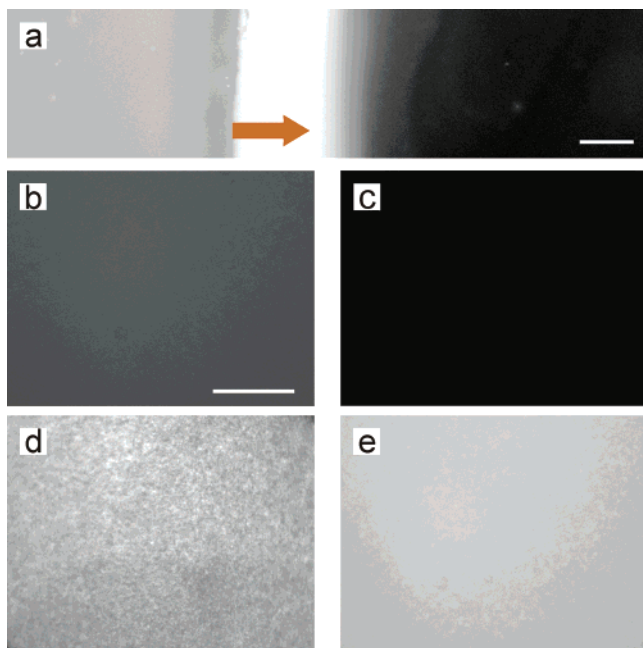


Figure 6. (a) Epifluorescence image of the patterned lipid bilayer edge (eggPC with 1.0 mol % Texas Red DHPE) on 184-PDMS oxidized for ~ 15 s while masked with a 5-mm-diameter polypropylene mask. The orange arrow points from the edge of the mask to the mask's interior. The scale bar is $250 \mu\text{m}$. (b–e) Magnified epifluorescence images of the interior masked region on PDMS after (b) ~ 5 , (c) ~ 15 , (d) ~ 45 , and (e) ~ 120 s of exposure to air plasma, removal of mask, and addition of eggPC with 1% Texas Red SUVs. The scale bar is $25 \mu\text{m}$.

spot photobleaching,³⁶ their fluorescence intensity, and their appearance under high magnification. Frequently, the interior of the masked region had a different lipid structure than the edge of the mask. In these cases, the interior lipid phase was always one that formed with less plasma oxidation than the lipid structure at the mask edge. For example (Figure 6a), we observed gap regions in the interior of the mask and adsorbed vesicles at the edge of the mask but never the reverse.

The ability to form large regions that support a single lipid phase allowed direct characterization of the surface chemistry of these regions by contact angle measurements. For the polymerization and curing conditions used herein, unoxidized PDMS had a contact angle of 113° , while patterned PDMS that supported monolayers showed a contact angle of 109 – 110° . Gap regions formed on PDMS with a contact angle of 98 – 100° , while adsorbed vesicles corresponded to a contact angle of 60 – 62° . Fluid supported bilayers formed on PDMS with a relatively wide range of contact angles, with the upper limit being approximately 30° and the most frequent one being 20° . This one-to-one correspondence between the contact angle and the supported lipid phase indicates that different supported lipid phases form in response to different PDMS surface chemistries.

Generally, the effects of plasma oxidation on PDMS depend highly on the degree of cross-linking in the polymer, the type of plasma used, the separation of the PDMS surface and the electrodes, the exposure time, the power, and so forth. Because of the unusual conditions used for these studies, there is no existing precedent to relate the masked PDMS plasma oxidation times and

contact angles to PDMS surface chemistry. To our knowledge, the most comparable report is from Hillborg et al.³³ in which contact angle and X-ray photoelectron spectroscopy data are presented for PDMS that had been oxidized in air plasma for varying amounts of times. The authors report that with increasing air plasma oxidation time, the amount of Si bonded to three and four oxygens (SiO_x) increases relative to Si bonded to two oxygens (unoxidized PDMS) and that the ratio of oxygen to carbon increases. They also conclude that the different Si–O species are mixed on the submicrometer scale. Several of our observations show the same trend as observed by Hillborg et al. We observe contact angles (100 and 60°) corresponding to intermediate hydrophilic/hydrophobic character, suggesting that PDMS surfaces oxidized to an intermediate extent are a mixture of surface groups rather than a single chemical species. Although it is possible to form supported bilayer patches $1 \mu\text{m}^2$ in area,¹⁴ we do not observe coexisting patches of different supported-lipid phases. Therefore, we suggest that the surface chemistry of PDMS oxidized at an intermediate level is one of $\text{SiO}(\text{CH}_3)_2$ and SiO_x mixed on the submicrometer scale.³⁷ By correlating our measured contact angles with those of Hillborg et al., we speculate that surfaces corresponding to gap, adsorbed vesicle, and bilayer regions are composed of on the order of 5% SiO_x , 20% SiO_x , and between 35 and 60% SiO_x , respectively.

From a general point of view the most important finding of our study is that the surface chemistry of a substrate can be modified such that a variety of different lipid structures, including no lipid assembly, can be supported on the surface one at a time. Sufficient plasma oxidation transforms hydrophobic PDMS (on which monolayers form) to a surface that is hydrophilic enough for bilayer formation.³⁹ However, in contrast to the results from Silin et al.,²³ this transformation is not continuous. No lipids adhere to PDMS with a contact angle of approximately 100° ,⁴⁰ whereas for a similar lipid composition and surface wettability, Silin et al. observe significant lipid adsorption. With somewhat longer plasma oxidation times,⁴¹ the presence of adherent vesicles indicates that the adhesion potential is strong enough to bind vesicles but too weak to lead to rupture of vesicles and formation of a supported bilayer.

These findings have important theoretical consequences. Lipid adhesion depends crucially on the chemical composition of the surface. Bilayers only form on very

(37) Silicone oligomers are known to gradually migrate to the surface of PDMS after plasma oxidation. These oligomers have a water contact angle of $\sim 108^\circ$ and form supported lipid monolayers upon exposure to lipid vesicles.³⁸ The oxidized PDMS surfaces used herein remain hydrophilic for many hours, suggesting that these oligomers are not present in significant quantities on the PDMS surface on that time scale. If an oxidized PDMS substrate (which normally would support a lipid bilayer) is allowed to recover in air for 24 h, the surface approaches its initial hydrophobicity and forms a supported monolayer when exposed to lipid vesicles.

(38) Glasmastar, K.; Gold, J.; Andersson, A.; Sutherland, D. S.; Kasemo, B. *Langmuir* **2003**, *19*, 5475.

(39) On hydrophobic PDMS, monolayer formation is most probably driven by the hydrophobic interaction between the hydrophobic lipid tails and the SiCH_3 -terminated substrate in the presence of water. On hydrophilic PDMS, the direct or water-mediated interactions between the SiO_x groups and the hydrophilic lipid heads are strong enough to lead to vesicle rupture.

(40) This suggests that the presence of a small number of polar SiO_x groups is sufficient to prevent monolayer adsorption (by weakening the hydrophobic interaction) while being insufficient to drive adsorption of lipid heads on SiO_x groups.

(41) In fact, it might be difficult to experimentally distinguish between no lipid adhesion and weak vesicle adhesion because for weak adhesion potentials already shear rates in the surrounding liquid of the order of $1/\text{s}$ can lead to detachment of vesicles from the substrate [Seifert, U. *Phys. Rev. Lett.* **1999**, *83*, 876].

(36) The bilayer regions typically recovered somewhat faster than the monolayer regions. Typical diffusion coefficients were $D = 1.7 \mu\text{m}^2/\text{s}$ for the bilayer and $D = 0.9 \mu\text{m}^2/\text{s}$ for the monolayer.

hydrophilic surface regions. Thus, the adhesion behavior of bilayers differs significantly from that of conventional liquids, such as, for example, water. In those systems, the thickness and morphology of the wetting layer depend continuously on the roughness and chemical structure of the substrate. For example, droplets of a conventional liquid always wet chemically structured substrates; that is, they always form droplets. Only their precise morphology is determined by the boundary conditions corresponding to the substrate structure.⁴² However, bilayer adhesion appears to be a rather discontinuous process, which either takes place or not. Novel theoretical approaches might be necessary to model this phenomenon

(42) Lenz, P.; Lipowsky, R. *Phys. Rev. Lett.* **1998**, *80*, 1920.

(43) Swain, P. S.; Andelman, D. *Langmuir* **1999**, *15*, 8902. Swain, P. S.; Andelman, D. *Phys. Rev. E* **2001**, *63*, 051911.

because classical descriptions of membrane adhesion (such as, e.g., the Deryagin approximation) predict that chemical patterning of substrates enhances bilayer formation.⁴³

Acknowledgment. P.L. thanks all members of the Boxer group for their kind hospitality. The help and advice of Jennifer Hovis, Joe Johnson, Lance Kam, Li Kung, and Fred Rosell are gratefully acknowledged. Special thanks to Chris Ackerson for his advice on EM-grids. This work is supported in part by a grant from the NSF Biophysics Program, by the NIH, and by the MRSEC Program of the NSF under Award No. DMR-0213618. P.L. acknowledges financial support through an Emmy Noether-fellowship of the Deutsche Forschungsgemeinschaft (Le 1214/1-1).

LA048450I